

Proximity induced spin-valley polarization in silicene/germanene on F-doped WS₂

Shahid Sattar, Nirpendra Singh, and Udo Schwingenschlög^{*}

King Abdullah University of Science and Technology (KAUST),

Physical Science and Engineering (PSE) Division, Thuwal 23955-6900, Saudi Arabia

Abstract

Silicene and germanene are key materials for the field of valleytronics. However, interaction with the substrate, which is necessary to support the electronically active medium, becomes a major obstacle. In the present work, we propose a substrate (F-doped WS₂) that avoids detrimental effects and at the same time induces the required valley polarization, so that no further steps are needed for this purpose. The behavior is explained by proximity effects on silicene/germanene, as demonstrated by first-principles calculations. Broken inversion symmetry due to the presence of WS₂ opens a substantial band gap in silicene/germanene. F doping of WS₂ results in spin polarization, which, in conjunction with proximity-enhanced spin orbit coupling, creates sizable spin-valley polarization.

Keywords: silicene, germanene, proximity effect, spintronics, valleytronics

^{*} udo.schwingenschlogl@kaust.edu.sa, +966(0)544700080

I. INTRODUCTION

Silicene and germanene are topological insulators with nontrivial band gaps of 2 meV and 24 meV, respectively, induced by spin orbit coupling (SOC) [1]. The band gap can be controlled electrically by applying a gate voltage in the out-of-plane direction [2]. It is anticipated that both materials host quantum spin Hall [3], quantum anomalous Hall [4], and valley polarized quantum anomalous Hall [5] phases. Silicene has been prepared on various substrates [6–9], while it is questionable whether it can exist in freestanding form (which also applies to germanene). This is the reason why various theoretical results on the interaction with possible substrates are found in the literature, including the insulator h -BN [10], the semiconductor GaAs [11], and the metals Ca [12], Ag [13], and Ir [14]. While on metallic substrates the Dirac behavior of silicene typically is not maintained [15, 16], transition metal dichalcogenides are characterized by a weak interaction [17]. From a different perspective, the latter class of materials is receiving great interest in recent days due to the fact that it realizes band gaps in a technologically attractive range [18]. Transition metal dichalcogenides also have proven to be suitable hosts for graphene [19, 20] and it has been demonstrated that the SOC of graphene can be enhanced by three orders of magnitude to about 17 meV on WS_2 due to proximity effects [21].

Valleytronics is emerging as a new and exciting area of research, aiming to exploit the valley degree of freedom in Dirac materials [22, 23]. An essential prerequisite of valleytronics, of course, is the availability of materials with valley polarization, i.e., the energetical degeneracy of the valleys at the high symmetry K and K' points of the hexagonal Brillouin zone must be lifted. While this is difficult to realize in graphene, the stronger SOC and buckled lattice of silicene/germanene provide an avenue to access and control the valley degree of freedom [24]. Spin and valley polarization can be achieved by means of doping and decoration with certain 3d or 4d transition metals [25, 26] as well as by an external electric field [4, 5, 27]. However, interaction with the substrate is typically detrimental, because the electronic states are perturbed [28]. Besides the need to reduce the interaction with the substrate, it would be a great advantage if the substrate itself can be used to induce the required valley polarization, in order to reduce the complexity of the system. In this context, we show in the present work that proximity effects between silicene/germanene and WS_2 can be utilized to obtain a suitable platform to explore spin and valley physics. We

first discuss the band characteristics and spin splitting in silicene/germanene induced by the strong SOC in WS_2 and afterwards demonstrate that the spin polarization in F-doped WS_2 generates spin-valley polarization.

II. COMPUTATIONAL METHOD

We use the Vienna Ab-initio Simulation Package to perform first-principles calculations based on density functional theory [29]. The exchange correlation potential is described in the generalized gradient approximation, using the Perdew-Burke-Ernzerhof scheme, and the plane wave cutoff energy is set to a sufficiently large value of 475 eV. Moreover, the SOC is taken into account in all calculations and the van der Waals interaction is incorporated using the DFT-D3 method [30]. The optimized lattice constants of silicene, germanene, and WS_2 are 3.86 Å, 4.05 Å, and 3.18 Å. In order to reduce the lattice mismatch to 2.9% and 1.9%, respectively, a $4 \times 4 \times 1$ supercells of silicene and germanene are placed on top of a $5 \times 5 \times 1$ supercell of WS_2 . Vacuum slabs of 15 Å thickness are used to obtain two-dimensional models. For the Brillouin zone integration, Monkhorst-Pack $1 \times 1 \times 1$ and $3 \times 3 \times 1$ k-meshes are employed in the structure relaxations and band structure calculations, respectively. We achieve in each case at least an energy convergence of 10^{-6} eV and an atomic

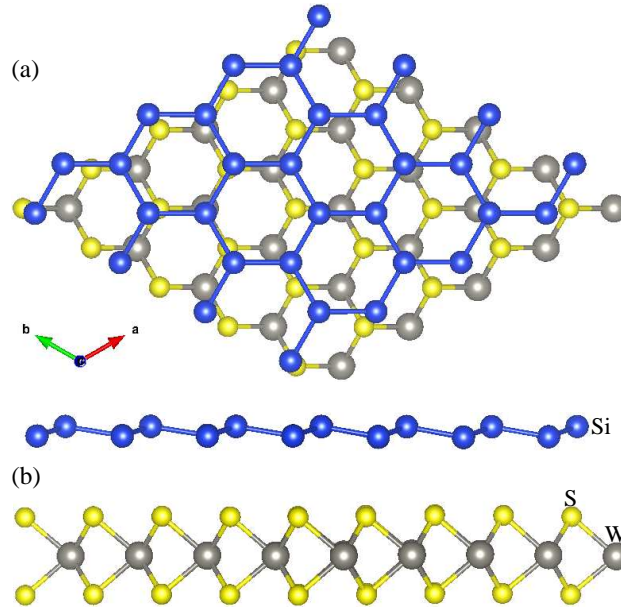


FIG. 1. Silicene on monolayer WS_2 : (a) top view and (b) side view.

force convergence of 10^{-2} eV/Å.

III. RESULTS AND DISCUSSION

The optimized crystal structure of silicene on top of monolayer WS₂ is illustrated in Fig. 1. A corresponding figure for germanene looks very similar and therefore is not shown. For different stackings of silicene/germanene on top of WS₂ (different lateral shifts) we obtain very small (few meV) total energy differences, showing that the materials can easily slide on each other. The distance between the two component materials turns out to be 3.13 Å in the case of silicene and 2.90 Å in the case of germanene. While the buckling of silicene is hardly affected by the interaction with WS₂ (0.46 Å), it is slightly enhanced to 0.74 Å for germanene (0.65 Å in the freestanding case). The smaller interlayer distance and the enhancement of the buckling demonstrate that WS₂ interacts more with germanene than with silicene, though the coupling is still weak. In order to quantify the interaction, we calculate the binding energy $(E_{\text{silicene/germanene}+\text{WS}_2} - E_{\text{silicene/germanene}} - E_{\text{WS}_2})/N$, given by the total energies of the combined system, freestanding silicene/germanene, and freestanding monolayer WS₂. Furthermore, N is the number of Si/Ge atoms. We obtain values of -158 meV and -171 meV for silicene and germanene, respectively, confirming our conclusion that the interaction is stronger in the latter case.

The electronic band structures in Fig. 2 show that both silicene and germanene on WS₂ maintain a linear dispersion of the π bands in the vicinity of the Fermi energy. This is the case both when the SOC is neglected and when it is taken into account. Without SOC we obtain band gaps of 29 meV and 38 meV, see Fig. 2(a/c), for silicene and germanene on WS₂, respectively, which is comparable to the thermal energy at room temperature. The reason for the opening of a band gap is the broken inversion symmetry in the presence of WS₂. SOC lifts the spin degeneracy at the K and K' points and results in spin splittings of 8 meV and 32 meV in the valence band of silicene and germanene, respectively, and 3 meV and 19 meV in the conduction band, see Fig. 2(b/d). The effect of the SOC is enhanced in the presence of WS₂ as a consequence of tiny hybridization between the Si/Ge p and W d orbitals. WS₂ indeed is characterized by very strong SOC, as reflected by spin splittings of 431 meV (valence band) and 29 meV (conduction band) in a freestanding monolayer [31]. The enhancement mechanism by proximity SOC is similar to the case of graphene

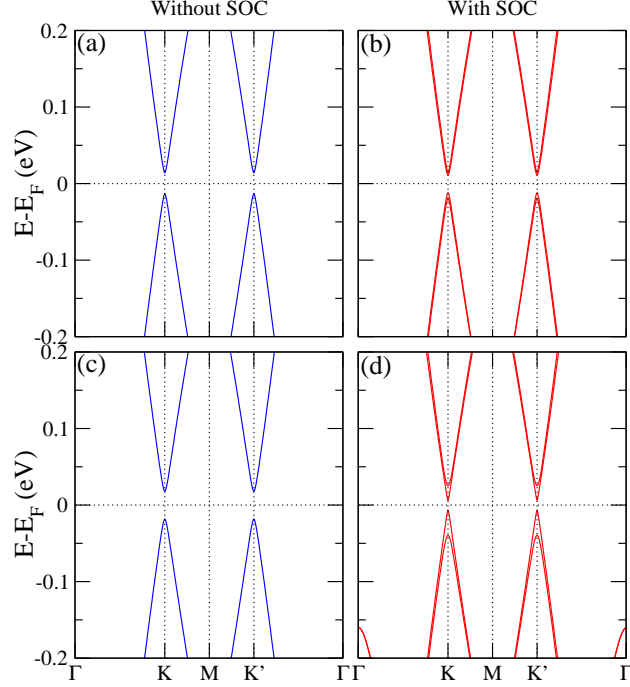


FIG. 2. Band structures of (a/b) silicene and (c/d) germanene on monolayer WS_2 . The SOC is neglected (left) or taken into account (right).

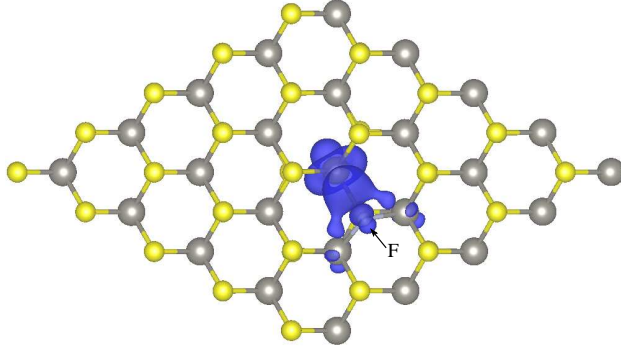


FIG. 3. Spin density in F-doped WS_2 .

on transition metal dichalcogenides [32], but due to the buckling of silicene/germanene the magnitude of spin splitting here is different in the valence and conduction bands. As a consequence of the lifted spin degeneracy, we obtain reduced band gaps of 23 meV and 14 meV for silicene and germanene on WS_2 , respectively.

In the following we will argue that silicene/germanene on F-doped WS_2 develops energetically inequivalent band edges at the K and K' points, i.e., spin-valley polarization. The advantage of doping the substrate instead of the electronically active material (the material

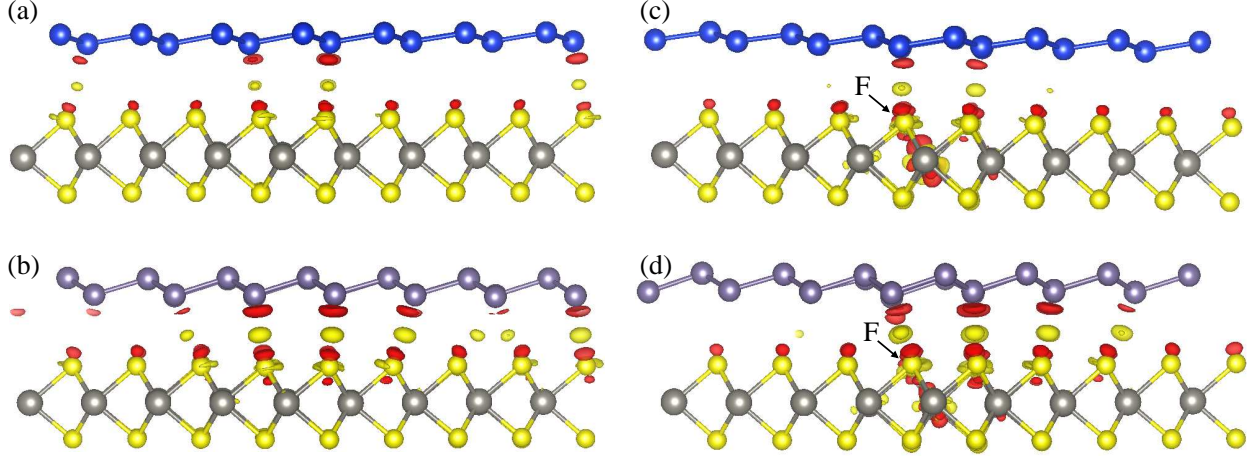


FIG. 4. Charge density difference induced by interaction of (a/b) silicene/germanene with monolayer WS_2 . Corresponding results for interaction with F-doped WS_2 are given in (c/d). Yellow and red colors represent charge accumulation and depletion, respectively. The plot takes into account the Si/Ge p , W d , and S p states, showing the 9×10^{-4} electrons/Bohr³ isosurface.

giving rise to the states close to the Fermi energy) is that impurity scattering is avoided. Specifically, we replace one S atom in the $5 \times 5 \times 1$ supercell of WS_2 with an F atom, corresponding to a doping concentration of 2%, in order to simulate the dilute doping limit. An earlier study has shown that substitutional F doping at the S site is possible in MoS_2 [33]. We calculate the binding energies $E(\text{WS}_2, \text{vac}) + E(\text{X}) - E(\text{WS}_2, \text{X})$ and obtain values of 4.3 eV for $\text{X} = \text{F}$ and 6.1 eV for $\text{X} = \text{S}$, where $E(\text{WS}_2, \text{vac})$ is the energy of a relaxed WS_2 monolayer with one S vacancy, $E(\text{X})$ is the energy of an X atom, and $E(\text{WS}_2, \text{X})$ is the energy of a relaxed WS_2 monolayer with one S atom replaced by an X atom. Since the binding energies of F and S are similar, it is likely that substitutional F doping at the S site is also possible in WS_2 . Experimental support for this conclusion comes from the realization of P doping in MoS_2 and WSe_2 [34, 35] and Cl doping in MoS_2 and WS_2 [36]. By comparing spin degenerate and polarized calculations for the doped supercell, we obtain an energy gain of 134 meV in the spin polarized case and a total magnetic moment of $1 \mu_B$. Next to the F atom the charge transfer from the three neighbouring W atoms is reduced from two electrons to one electron (F^{-1} state instead of S^{-2} state). The remaining electron is located on one of the three W atoms and gives rise to the spatial distribution of spin density shown in Fig. 3. We obtain a small F magnetic moment of $0.05 \mu_B$, which is also reflected by Fig. 3.

We obtain for silicene and germanene on top of F-doped WS_2 smaller distances between

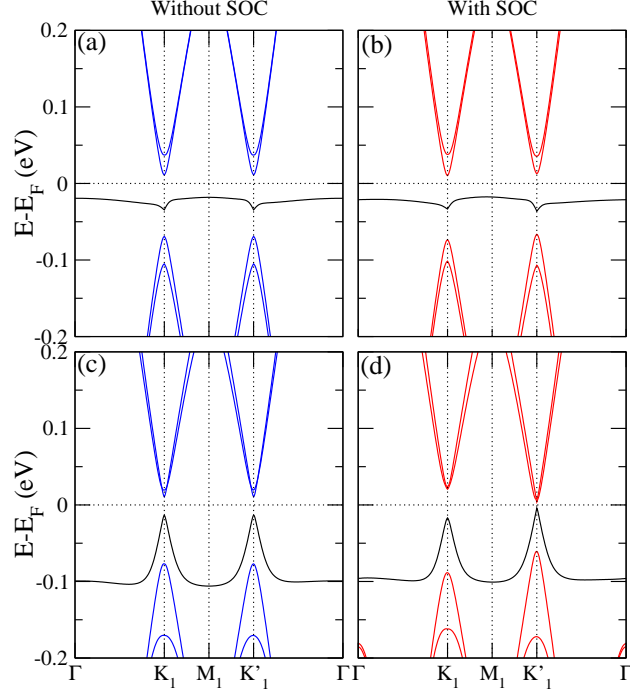


FIG. 5. Band structures of (a/b) silicene and (c/d) germanene on F-doped monolayer WS_2 . The SOC is neglected (left) or taken into account (right). The F impurity band is shown in black color.

the component materials, 3.06 Å and 2.79 Å, respectively, as compared to the case of pristine WS_2 . This fact can be attributed to the additional magnetic coupling. A comparison of the interaction in the cases of pristine and F-doped WS_2 is given in Fig. 4 in terms of charge density difference plots. While the charge redistribution in the van der Waals gap is only slightly modified after F doping, compare the top to the bottom row of Fig. 4, the dopant atom is strongly affected, supporting the idea of magnetic coupling. We obtain still a total magnetic moment of 1 μ_B , carried largely by one W atom. This atom realizes a larger distance (2.70 Å) to the F atom than the other two neighbouring W atoms (2.30 Å), very similar to the situation without silicene/germanene. In addition, the F magnetic moment is reduced to 0.05 μ_B . The band structure of silicene/germanene shows significant alterations in contact with F-doped WS_2 , see Fig. 5. Without SOC, the spin splitting in the valence band is enhanced to 36/91 meV and that in the conduction band to 25/9 meV. This fact is expected to simply reduce the band gaps, however, we observe in both cases the creation of an in-gap band just below the Fermi energy. Analysis of the orbital character of this band shows that it arises almost purely from the F impurity.

Broken time-reversal symmetry due to the spin polarization in F-doped WS_2 induces

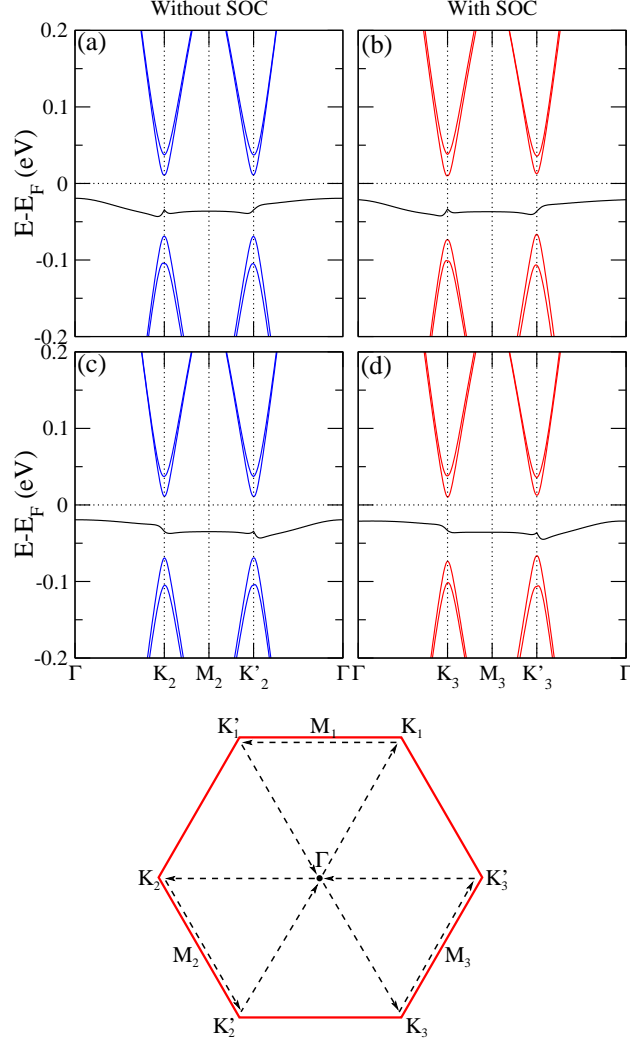


FIG. 6. Band structures of silicene on F-doped monolayer WS_2 for the 2 K and 2 K' points not covered by Fig. 5(a/b). The SOC is neglected (left) or taken into account (right). The F impurity band is shown in black color. **The different Brillouin zone paths are highlighted by dashed arrows (bottom).**

spin-valley polarization in silicene/germanene when the SOC is taken into account, see Fig. 5(b/d). Specifically, the spin splitting in the valence/conduction band (not counting the F impurity band) is smaller/larger at the K than at the K' point. For silicene we obtain values of 28 meV and 40 meV for the valence band and 27 and 24 meV for the conduction band, respectively. More importantly, valley polarization of 7 meV is created in the silicene valence band and one of 2 meV in the conduction band. For germanene these effects are enhanced, with spin splittings of 74 meV and 111 meV (valence band) as well as 4 meV

and 5 meV (conduction band) at the K and K' points, respectively. The valley polarization here amounts to 28 meV and 16 meV for the germanene valence and conduction bands, respectively, which opens a route to spin-valley polarization even at room temperature. In order to demonstrate that the K and K' valleys are virtually not affected by the symmetry breaking in F-doped WS₂, as they belong almost purely to silicene/germanene, we show in Fig. 6 for the silicene system the band structures of the 2 K and 2 K' points not covered by Fig. 5(a/b). We observe no lifting of the valley degeneracy in the case without SOC and exactly the same valley structure as before in the case with SOC. We also have checked that the spin hybridization at the valleys is negligible. Moreover, while the F impurity band is located next to the Fermi energy, the F states are spatially separated from the Si/Ge states and therefore do not limit exploitation of the spin-valley polarization.

In conclusion, we have demonstrated that silicene and germanene in proximity to monolayer WS₂ develop sizeable band gaps (due to inversion symmetry breaking) and spin splittings (due to proximity SOC). F doping of WS₂ results in spin polarization with a total magnetic moment of 1 μ_B , since the charge transfer from the three neighbouring W atoms is reduced. The remaining spin polarized electron is largely located on one W atom. Our main finding is that F-doped WS₂ makes it possible to achieve substantial spin-valley polarization in silicene and germanene. In contrast to silicene, germanene even can enable valleytronics devices operating at ambient conditions.

ACKNOWLEDGMENTS

The research reported in this publication was supported by funding from King Abdullah University of Science and Technology (KAUST).

-
- [1] S. Cahangirov, M. Topsakal, E. Aktürk, H. Sahin, and S. Ciraci, Phys. Rev. Lett. **102**, 236804 (2009).
 - [2] Z. Ni, Q. Liu, K. Tang, J. Zheng, J. Zhou, R. Zin, Z. Gao, D. Yu, and J. Lu, Nano Lett. **12**, 113 (2012).
 - [3] C. C. Liu, W. Feng, and Y. Yao, Phys. Rev. Lett. **107**, 076802 (2011).
 - [4] M. Ezawa, Phys. Rev. Lett. **109**, 055502 (2012).

- [5] H. Pan, Z. Li, C. C. Liu, G. Zhu, Z. Qiao, and Y. Yao, Phys. Rev. Lett. **112**, 106802 (2014).
- [6] P. Vogt, P. D. Padova, C. Quaresima, J. Avila, E. Frantzeskakis, M. C. Asensio, A. Resta, B. Ealet, and G. Le Lay, Phys. Rev. Lett. **108**, 155501 (2012).
- [7] L. Chen, C. C. Liu, B. Feng, X. He, P. Cheng, Z. Ding, S. Meng, Y. Yao, and K. Wu, Phys. Rev. Lett. **109**, 056804 (2012).
- [8] A. Fleurence, R. Friedlein, T. Ozaki, H. Kawai, Y. Wang, and Y. Y. Takamura, Phys. Rev. Lett. **108**, 245501 (2012).
- [9] L. Tao, E. Cinquanta, D. Chiappe, C. Grazianetti, M. Fanciulli, M. Dubey, A. Molle, and D. Akinwande, Nat. Nanotechnol. **10**, 227 (2015).
- [10] Z. X. Guo, S. Furuya, J. Iwata, and A. Oshiyama, Phys. Rev. B **87**, 235435 (2013).
- [11] A. Bhattacharya, S. Bhattacharya, and G. P. Das, Appl. Phys. Lett. **103**, 123113 (2013).
- [12] P. Pflugradt, L. Matthes, and F. Bechstedt, New J. Phys. **16**, 075004 (2014).
- [13] Z. X. Guo, S. Furuya, J. I. Iwata, and A. Oshiyama, J. Phys. Soc. Jpn. **82**, 063714 (2013).
- [14] L. Meng, Y. Wang, L. Zhang, S. Du, R. Wu, L. Li, Y. Zhang, G. Li, H. Zhou, W. A. Hofer, and H. J. Gao, Nano Lett. **13**, 685 (2013).
- [15] S. Cahangirov, M. Audiffred, P. Tang, A. Iacomino, W. Duan, G. Merino, and A. Rubio, Phys. Rev. B **88**, 035432 (2013).
- [16] C. L. Lin, R. Arafune, K. Kawahara, M. Kanno, N. Tsukahara, E. Minamitani, Y. Kim, M. Kawai, and N. Takagi, Phys. Rev. Lett. **110**, 076801 (2013).
- [17] N. Gao, J. C. Li, and Z. Jiang, Phys. Chem. Chem. Phys. **16**, 11673 (2014).
- [18] Q. H. Wang, K. K. Zadeh, A. Kis, J. N. Coleman, and M. S. Strano, Nat. Nanotech. **7**, 699 (2012).
- [19] C. P. Lu, G. Li, K. Watanabe, T. Taniguchi, and E. Y. Andrei, Phys. Rev. Lett. **113**, 156804 (2014).
- [20] T. Georgiou, R. Jalil, B. D. Belle, L. Britnell, R. V. Gorbachev, S. V. Morozov, Y. J. Kim, A. Gholinia, S. J. Haigh, O. Makarovskiy, L. Eaves, L. A. Ponomarenko, A. K. Geim, K. S. Novoselov, and A. Mishchenko, Nat. Nanotech. **8**, 100 (2013).
- [21] A. Avsar, J. Y. Tan, T. Taychatanapat, J. Balakrishnan, G. K. W. Koon, Y. Yeo, J. Lahiri, A. Carvalho, A. S. Rodin, E. C. T. O'Farrell, G. Eda, A. H. Castro Neto, and B. Özyilmaz, Nat. Commun. **5**, 4875 (2014).
- [22] A. Rycerz, J. Tworzydło, and C. W. J. Beenakker, Nat. Phys. **3**, 172 (2007).

- [23] D. Xiao, W. Yao, and Q. Niu, Phys. Rev. Lett. **99**, 236809 (2007).
- [24] M. Ezawa, Phys. Rev. B **87**, 155415 (2013).
- [25] X. L. Zhang, L. F. Liu, and W. M. Liu, Sci. Rep. **3**, 2908 (2013).
- [26] J. Zhang, B. Zhao, and Z. Yang, Phys. Rev. B **88**, 165422 (2013).
- [27] W. F. Tsai, C. Y. Huang, T. R. Chang, H. Lin, H. T. Jeng, and A. Bansil, Nat. Commun. **4**, 1500 (2013).
- [28] M. Satta, S. Colonna, R. Flammini, A. Cricenti, and F. Ronci, Phys. Rev. Lett. **115**, 026102 (2015).
- [29] G. Kresse and D. Joubert, Phys. Rev. B: Condens. Matter **59**, 1758 (1999).
- [30] S. Grimme, J. Antony, S. Ehrlich, and H. Krieg, J. Chem. Phys. **132**, 154104 (2010).
- [31] Y. C. Cheng, Z. Y. Zhu, M. Tahir, and U. Schwingenschlögl, EPL **102**, 57001 (2013).
- [32] M. Gmitra, D. Kochan, P. Högl, and J. Fabian, Phys. Rev. B **93**, 155104 (2016).
- [33] K. Dolui, I. Rungger, C. D. Pemmaraju, and S. Sanvito, Phys. Rev. B **88**, 075420 (2013).
- [34] E. Kim, C. Ko, K. Kim, Y. Chen, J. Shuh, S.-G. Ryu, K. Wu, X. Meng, A. Suslu, S. Tongay, J. Wu, and C. P. Grigoropoulos, Adv. Mater. **28**, 341 (2016).
- [35] A. Nipane, D. Karmakar, N. Kaushik, S. Karande, and S. Lodha, ACS Nano **10**, 2128 (2016).
- [36] L. Yang, K. Majumdar, H. Liu, Y. Du, H. Wu, M. Hatzistergos, P. Y. Hung, R. Tieckelmann, W. Tsai, C. Hobbs, and P. D. Ye, Nano Lett. **14**, 6275 (2014).